International Journal of Technology 13(8) 1612-1621 (2022)
Received August 2022 / Revised December 2022 / Accepted December 2022

International Journal of Technology

http://ijtech.eng.ui.ac.id

Fabrication of Rigid Polyurethane Foam Lumbar Spine Model for Surgical Training using Indirect Additive Manufacturing

Asriyanti[1,2], Kushendarsyah Saptaji[1*], Nisa Khoiriyah[1,2], Muhammad Satrio Utomo[3,4], Made Subekti Dwijaya[3], Muhammad Hanif Nadhif[4], Farid Triawan[1]

[1]Mechanical Engineering Department, Faculty of Engineering and Technology, Sampoerna University, Jl. Raya Pasar Minggu No. Kav. 16, Jakarta 12780 Indonesia
[2]Department of Aerospace and Mechanical Engineering, The University of Arizona, Tucson, AZ 85721, United States
[3]National Agency for Research and Innovation, Kawasan PUSPIPTEK, Banten 15314 Indonesia
[4]Faculty of Medicine, Universitas Indonesia, Jakarta 10430 Indonesia

Abstract. Lumbar model is an artificial bone that is commonly used in surgical training to simulate working with the human-like bone for the trainer. The common lumbar model is made of rigid polyurethane (PU) foam and is produced using casting. However, the current lumbar model is expensive and has limitations in representing the real human lumbar, especially in geometry, visuals, and haptics. Therefore, an alternative method of fabricating lumbar models made of rigid polyurethane for surgical training using indirect additive manufacturing will be investigated in this paper. The proposed indirect additive manufacturing is a combination of 3D printing and casting methods. The main process of this method is started by fabricating a mold made of polyvinyl alcohol (PVA) using fused deposition modeling (FDM) 3D printing and subsequently casting PU foam material into the 3D printed PVA mold. Accordingly, the aim of this study is to find the optimized casting process parameters, especially for injecting the material into the mold, to achieve a better quality of lumbar model. The study was conducted using a Design of Experiment (DoE) Taguchi Orthogonal Array to optimize the casting process. The geometrical measurements of middle end-plate depth, upper end-plate width, spinal canal width, spinal canal depth, and lower pedicle length show the error ranged from 0.14% to 0.85%. The average porosity, measured from the body, lamina, and spinous, was found to be non-uniform. It is ranged from 19.58% to 21.94% on the middle part and 39.78% to 45.41% on the subsurface of lumbar model. The density was increased by 64.89% compared to the reference open molded PU foam.

Keywords: Indirect additive manufacturing; Lumbar spine model; Rigid polyurethane (PU) foam; Surgical training

1. Introduction

Lumbar is located at the lower part of the spine and has a function to support the upper body and protect the spinal cord (Frost et al., 2019). Due to its heavy functions, lumbar is prone to be injured and surgery is required to restore its function. As a result of the increasing use of lumbar surgery, a growing demand for lumbar spine model used in

*Corresponding author's email: kushendarsyah@sampoernauniversity.ac.id
doi: 10.14716/ijtech.v13i8.6125

surgical training is also increasing (Lewandrowski et al., 2020). Moreover, post-surgery monitoring is necessary to ensure the success of the surgical and implantation processes, such as in the dental implant system (Genisa et al., 2020).

There are several challenges in creating a lumbar spine model, and all the challenges lead to one fundamental issue where the models cannot accurately replicate the genuine parts in terms of visual, geometric, and haptic feedback. Various fabrication methods have been used to produce the lumbar spine model, such as machining, casting, and additive manufacturing. Machining is a traditional or subtractive manufacturing method used to make prostheses (Rani et al., 2017). This method is popular due to its low cost, high surface quality, and ease of use. However, this method is limited in the shapes that can be produced since it only moves in three axes for conventional machining and five axes for computer numerical control (CNC) machining (Kong et al., 2020). In addition, the machining process can also induce residual stress on the machined workpiece, which can initiate failure (Saptaji et al., 2019). The casting process is also widely used due to its ability to produce complex shapes with a variety of materials. However, the casting process is time consuming and has low dimensional accuracy, resulting in a low geometrical representation of the lumbar model (Lyashenko et al., 2018). In recent study, in order to improve the process efficiency and accuracy, additive manufacturing or 3D printing is being introduced due to its cost effectiveness, customizability, and able to build complex shaped model (Bai et al., 2019; Hanon et al., 2021). Fused Decomposition Modeling (FDM) is the most popular 3D printing method, in which the object is built layer by layer by using the extrusion method to melt the raw material in the form of filament, commonly made of polymer, through the nozzle (Hadisujoto et al., 2021; Mwema & Akinlabi, 2020). However, FDM is limited in the material used because the method does not support the printing process of the widely used material for the lumbar model (Clifton et al., 2019). Meanwhile, the material for the bone structure such as lumbar spine must have similar structure and properties (Saptaji et al., 2022). Rigid polyurethane (PU) foam is the most frequently used material. It is widely used in lumbar spine models due to its similarities with lumbar properties (Shim et al., 2012). Computational validation on thermoplastic polyurethane with lattice structure for intervertebral disc replacement also showed that the material is a suitable candidate (Nadhif et al, 2021). However, the fabrication of PU foam to become a lumbar model is only possible through the casting method, which is inefficient and has poor accuracy (Gama et al., 2018).

Due to all the challenges faced in fabricating lumbar model, an indirect additive manufacturing approach can be used to obtain a better quality of the lumbar spine model. Indirect additive manufacturing can be performed by combining FDM and casting processes to produce the part (Montero et al., 2020). The combination can be implemented since the desired material to fabricate the part is only possible through the casting process, meanwhile traditional casting process is not recommended due to its low accuracy and a long period of time required for mold preparation. Therefore, FDM can be used to produce the mold to improve efficiency and accuracy. The challenges in utilizing indirect additive manufacturing are located in determining the printing parameters and the process of injecting the material into the mold.

There are no studies reporting efforts to investigate and solve the optimization of the casting process, especially in the lumbar spine model fabrication. One of the challenges in casting PU foam is due to structure stabilization during the foaming and curing processes and its tendency to shrink (Rampf et al., 2011). The study in finding the optimal indirect additive manufacturing parameters, particularly during the casting process, is required in order to produce an excellent quality lumbar model. Therefore, the objective of this study is to find the optimized casting process parameters, especially for injecting the material into the mold. It is expected that a better quality of lumbar model can be achieved by evaluating the properties of a PU lumbar model fabricated using indirect additive manufacturing. The experimental work was conducted using Taguchi Orthogonal Arrays Design of Experiment (DoE). This method is commonly used to optimize the fabrication process by making some assumptions about factors and levels that have a significant effect on the issues (Mondal et al., 2020). The DoE was divided into two stages which are the optimization of printing parameters and casting processes.

2. Methods

2.1. Materials

Materials used in this study are water soluble polyvinyl alcohol (PVA) filament as the casting mold and rigid polyurethane (PU) foam as the material of the lumbar spine model. Rigid PU foam consists of part A (polyol) and part B (diisocyanate) with a ratio of 1:2 and a mixing time of 2.5 minutes (Sidek et al., 2017).

2.2. Tools

Several tools were used during this study, including software such as SolidWorks, Meshmixer, FlashPrint slicing software, ImageJ, and FlashForge Creator Pro 3D Printer. SolidWorks was used to design the samples. Meshmixer was used to modify the stereolithography (STL) file obtained from the patient's lumbar computerized tomography (CT) scan. FlashPrint was used to generate g-code that could be printed. ImageJ was used during the porosity characterization. A FlashForge Creator Pro 3D Printer with a nozzle diameter of 1.75 mm is used to print the PVA mold. The drilling tool is used to make holes in the mold for injection and excess PU foam during casting.

2.3. Experimental Procedures

2.3.1. Casting process optimization

The experiment was carried out based on the Design of Experiments (DoE) using Taguchi Orthogonal Arrays to determine the optimized parameters for the casting process. Preliminary findings and analysis show partially filled mold cavities occurred during casting of the PU foam due to the number of injections and excess (surplus) holes introduced to the PVA mold issue. Therefore, to ensure that PU foam can completely fill the mold cavity, the focus in DoE was to determine the number of injection and excess holes on the mold.

The experiment was initially performed by modifying the lumbar CT scan image data to become a lumbar mold using Meshmixer. CT scan image data is also useful in the analysis of a femoral bone fracture in the case of a sideways fall accident (Izmin et al., 2020). An initial experiment was performed prior to the 3D printing process of the mold to identify the best 3D printing parameter variations, particularly mold thickness and travel speed (Haque, 2020; Azhikannickal & Uhrin, 2019).The best travel speed was determined to be 70 mm/s, and the mold thickness was determined to be 2.4 mm. Meanwhile, the other printing parameters were determined based on the literature (Montero et al., 2020; Tagami et al., 2017), such as printing speed of 50 mm/s, extruder and platform temperatures of 205 ^{0}C and 45 ^{0}C, infill of 0%, layer height of 0.2 mm,

Table 1 Standard orthogonal array of DoE

Factor	Variation			
	1	2	3	4
Number of injection holes (In)	1	1	2	2
Number of excess holes (Exc)	2	4	2	4

Then, the lumbar mold made of PVA was sliced and printed. Subsequently, the printed lumbar mold was drilled to add injection and excess holes. The number of injection and excess holes varied from anterior body (In), spinous (In), articular process (Exc), and transverse process (Exc) based on the standard orthogonal array shown in Table 1. The injection and excess hole positions for the four variations are shown in Figure 1. The casting process was subsequently completed by injecting 9 mL of PU foam. The casting samples were then cured and undergone dissolution process to remove the PVA mold from the beaker glass to obtain the lumbar model. The workflow of the experimental setup is shown in Figure 2.

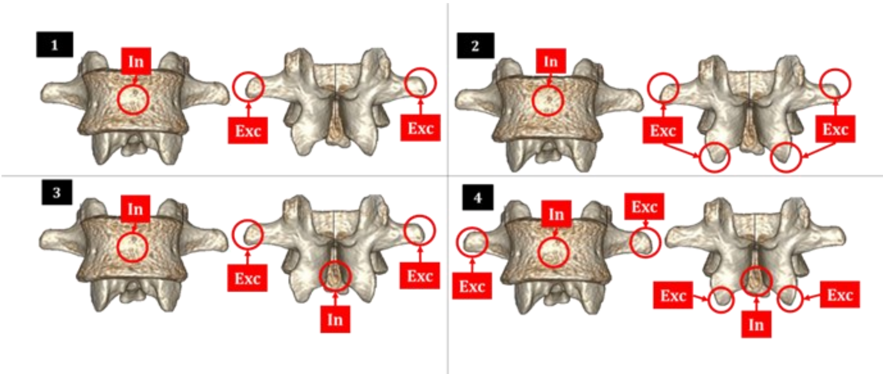

Figure 1 Locations of injection (In) holes and excess (Exc) holes for (1) Variation 1, (2) Variation 2, (3) Variation 3, (4) Variation 4 (Bozdag & Karaman, 2021)

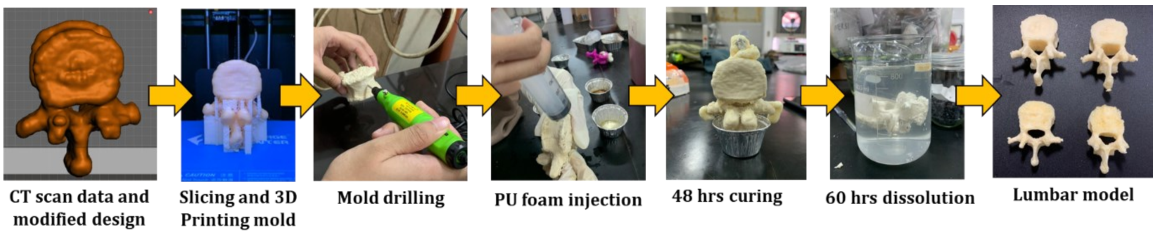

Figure 2 Experimental setup of lumbar model fabrication

2.3.2. Open molded PU foam

An open molded PU foam was fabricated as the reference properties of PU foam. It was used to compare the effect of indirect additive manufacturing on the PU foam properties. The specimen was prepared in an open aluminum cup that was used as a mold and allowed to foam freely. The procedure is shown in Figure 3.

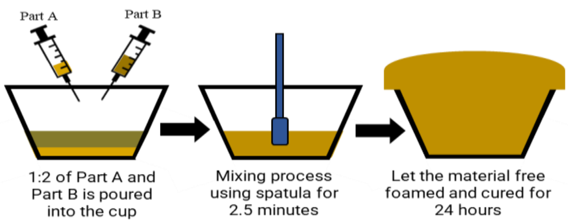

Figure 3 Illustration on the fabrication process of open molded PU foam

2.4. Characterization

2.4.1. Morphometry analysis

A morphometric analysis was conducted on evaluate the percent error to the desired dimension. A Vernier caliper with 0.05 accuracy was used to do the characterization. The dimensions of lumbar model between the CT scan data and fabricated lumbar model were compared in several parts, shown in Figure 4, including middle end-plate depth (EPDm), upper end-plate width (EPWn), spinal canal width (SCW), spinal canal depth (SCD), and lower pedicle length (PLI). The requirements of the error based on ASTM F1839 must be less than 5% (ASTM, 2014).

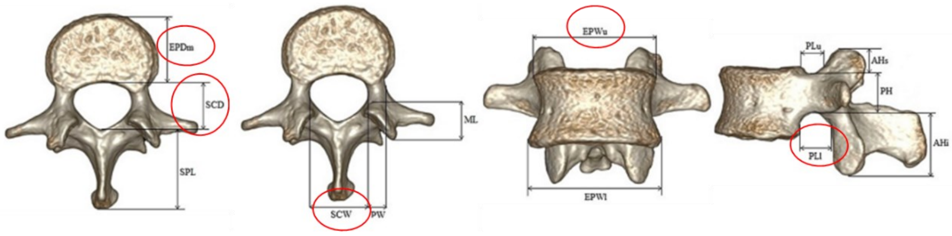

Figure 4 Locations of morphometry analysis performed for lumbar model (Bozdag & Karaman, 2021)

2.4.2. Porosity

The porosity of the lumbar model was assessed to evaluate the effect of the indirect additive manufacturing method on the uniformity of PU foam distribution. The sample preparation was based on ASTM F1839. A Motic BA310 Microscope with 5x magnification was used to capture the pore distribution in the subsurface and middle part of the lumbar body, lamina, and spinous. The lumbar model that undergone this measurement was limited to those who passed the morphometry analysis. The data obtained from the microscope was exported to ImageJ to measure the pore area. All the data at each location are summed and divided by the cross-sectional area to obtain the porosity.

2.4.3. Density measurement

Density measurement was conducted based on ASTM 1622 (ASTM, 2020) with the same samples characterized in porosity. It was used to see the effect of the indirect manufacturing process toward the change in the density of PU foam. The density was measured using the density formula, where the mass and volume must be obtained for each specimen. The mass was measured using a digital mass balance. Meanwhile, the volume was determined using the Archimedes method.

3. Result and Discussion

There were 12 lumbar models with 3 replications for each variation. The replications were produced in order to examine the consistency of the selected parameters. Figure 5 depicts a representative of each fabricated lumbar variation. During the casting process, it was found that PU foam was expanded throughout the excess holes. It shows that the mold has been completely filled with PU foam material, particularly in the pedicle area.. However, after the dissolution process to remove PVA mold, it was found that there are still some missing parts that have not formed in the lumbar model, even though the PU foam has raised throughout the excess holes. In general, variation 1 produced the perfect shape of the model with no missing parts as compared to other variations.

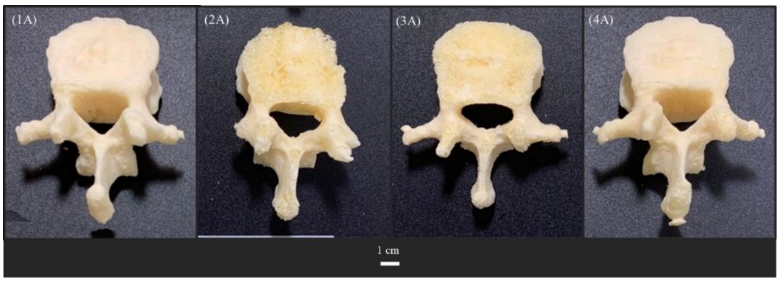

Figure 5 Superior view of PU foam lumbar model for (1A) Variation 1, (2A) Variation 2, (3A) Variation 3, (4A) Variation 4

3.1. Morphometry Analysis

The result of the morphometry analysis of 12 lumbar models, especially for EPDm, EPDu, SCW, SCD, and PLI, is shown in Figure 6. Based on the diagram, the percentage error of the lumbar model compared to the CT scan data is varied. In general, the percent error of variation 1 in every location is always below the percentage error limit, which ranges from 0.14% to 0.85%. In contrast, variation 2, variation 3, and variation 4 have some dimensions that exceed the error limit, ranging from 0.19% to 14.68%, 0.55% to 18.68%, 0.37% to 10.05%, respectively. Variation 2 is exceeded the error limit in EPDm and EPWu. Meanwhile, variation 3 surpasses the error limit in EPDm, EPWu, and SCD. Lastly, variation 4 exceeds the limit on EPWu and SCD.

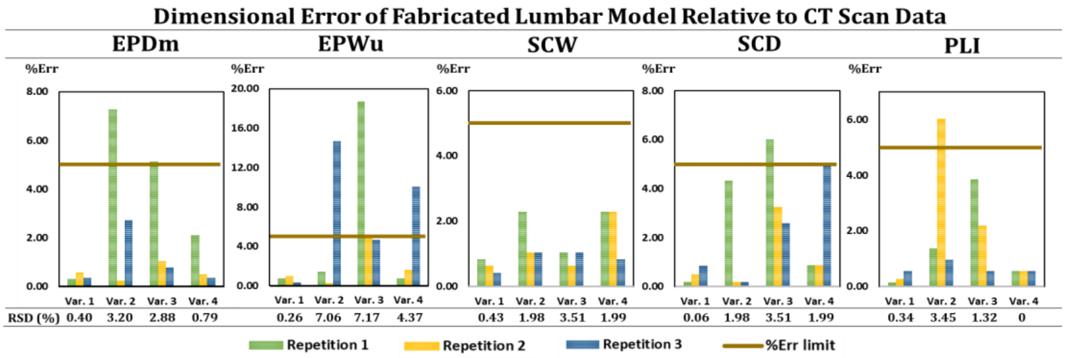

Figure 6 Dimensional error of fabricated lumbar model relative to CT scan data

The phenomenon where some variations exceeded the error limit are due to the missing parts on the lumbar model. For instance, in variation 2, there are some missing parts for every repetition on the lumbar body as shown in Figure 7. This missing part significantly increases the error in the EPWu dimension compared to the CT scan data. In this experiment, the casting process was performed by injecting PU foam to the mold from the anterior side vertically. As a result, the material was poured directly into the mold's bottom and raised to the interior side. However, due to the number and location of excess holes in the bottom, during the foaming process the material was prone go to the excess holes massively, resulted in mold pressure reduction (Lyashenko et al., 2018) and interparticle bonding strength between the material. Consequently, some parts of the lumbar model are fractured and collapsed during the dissolution of PVA mold.

The repeatability test was also performed on this characterization by considering the relative standard deviation (RSD). For all variations, the value of RSD is below 10% indicating that all variations are likely to have the same dimensions for every repetition. Accordingly, from this morphometry analysis, variation 1 shows the best result, in which the percent errors in dimension for every repetition are not exceeding the 5% limit.

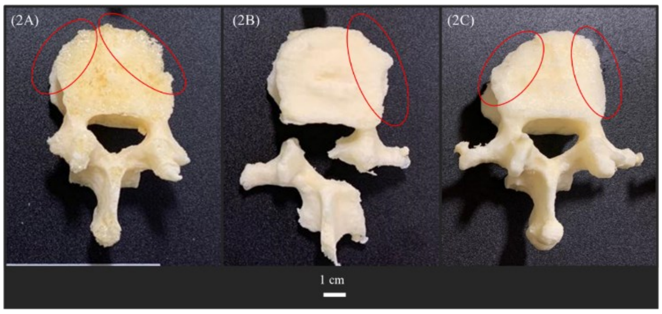

Figure 7 Variation 2 visual observations for (2A) repetition 1, (2B) repetition 2, (2C) repetition 3

The RSD result was better, with the highest value is only about 3.2% for variation 1, compared to a similar study about the fabrication process of hip joint using investment casting (Singh et al., 2014), where the value of RSD is up to 6.5%. In addition, the quality of the casting results is improved compared to a similar study about the fabrication of a spine model using the 3D printing method (Clifton et al., 2019), as can be observed from the lumbar structure and visual representation (Figure 8).

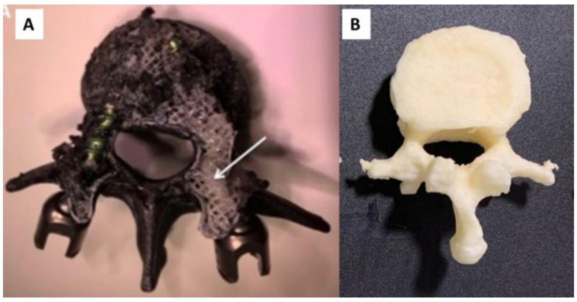

Figure 8 Comparision of lumbar spine model (A) Fabricated using 3D printing (Clifton et al., 2019), (B) Variation 1

3.2. Pore Distribution

Pore distribution analysis was used to evaluate the uniformity of the material by calculating the porosity of PU foam in the form of a lumbar model. There were 6 locations selected for the pore distribution analysis, including the lumbar body, lamina, and spinous. The pore distribution of each part was measured in the middle and subsurface, as shown in Figure 9 (a). The pores were measured using ImageJ, with the pore determination shown in Figure 9 (b). This analysis was only performed for variation 1 since it has a more complete shape of the model compared to other variations.

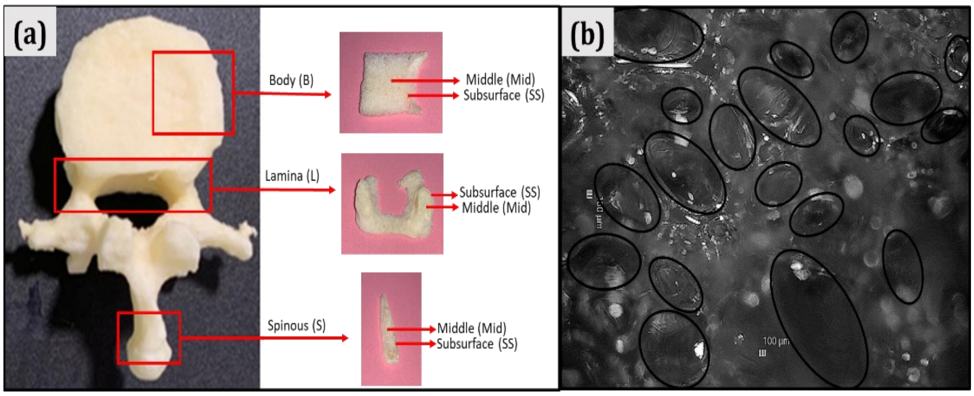

Figure 9 (a) Location of measured porosity, (b) Pores determination

Figure 10 (a) shows the consistency of porosity for repetition and measured location (middle and subsurface), respectively. The average porosities of the lumbar body's middle part, lamina, and spinous were 19.58% to 21.94%. Meanwhile, the average subsurface porosities on the same lumbar range from 39.78% to 45.41%. This phenomenon indicates that the density of each location on the lumbar model is not uniform considering the difference in porosity of middle and subsurface. Larger porosity implies that the location has a lower density (Gopinathan et al., 2021). In addition, the standard deviation at each location for all repetitions is below 10%, ranging from 1% to 8.57%.

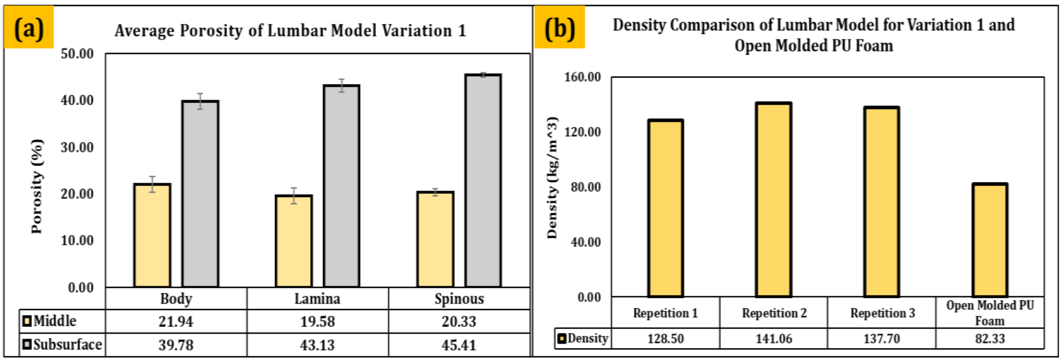

Figure 10 (a) Average porosity of lumbar model for Variation 1 **(b)** Density comparison of lumbar model for Variation 1 and open molded PU foam

3.3. Density Measurement

The density measurement was performed on Variation 1 with 3 replications. The density result for the whole lumbar is shown in Figure 10 (b). Based on the density measurement result, it shows that the density of PU foam in lumbar shape is increased compared to open molded PU foam. Compared to the average density for all repetitions, the density of the whole lumbar increases about 64.89%. The increase in density compared to the reference PU foam occurred due to the mold type. The reference PU foam was fabricated using an open mold, whereas the lumbar model was fabricated using close mold type. Accordingly, the material inside the lumbar mold is inhibited from being free foamed, which causes the packing effect (Jackovich et al., 2005), in which the void volume of the material becomes smaller (Wong & Kwan, 2008). As a result, the PU foam inside the lumbar mold is denser that the reference one. In addition, the repeatability test on the lumbar density shows that the RSD value is below 10%, which is 3.91%. It indicates that the variation of density is still acceptable according to the standard, and this variation can increase the physical properties of PU foam in terms of its density in the lumbar model.

4. Conclusions

In this study, the fabrication of a lumbar model using indirect additive manufacturing has been performed using a Taguchi orthogonal array. The lumbar mold made of PVA was successfully fabricated using an FDM 3D printer with no defects detected. This mold was utilized to produce the PU foam lumbar model. The variation in position and numbers of injecting holes and excess holes have a significant effect on the fabricated PU foam lumbar model. Variation 1 with one injecting hole located in the anterior body and two excess holes located in the transverse process, has successfully produced a perfect lumbar model with no missing parts. The morphometry analysis shows that the significant dimensions, namely middle end-plate depth (EPDm), upper end-plate width (EPWn), spinal canal width (SCW), spinal canal depth (SCD), and lower pedicle length (PLl) are below the percent error. The porosity also shows that variation 1 has a more uniform material distribution. In terms of density, it was found that the measured density was higher compared to the reference open molded PU foam.

References

ASTM, 2014. F1839 - 97: Standard Specification for Rigid Polyurethane Foam for use as a Standard Material for Testing Orthopaedic Devices and Instruments. In: *ASTM Book of Standards*, pp .6–11

ASTM, 2020. Standard Test Method for Apparent Density of Rigid Cellular Plastics In: *ASTM*

Book of Standards, pp. 4–7

Azhikannickal, E., Uhrin, A., 2019. Dimensional Stability Of 3D Printed Parts: Effects Of Process Parameters. *Ohio Journal of Science*, Volume 119(2), pp. 9–16

Bai, L., Gong, C., Chen, X., Sun, Y., Zhang, J., Cai, L., Zhu, S., Xie, S.Q., 2019. Additive Manufacturing Of Customized Metallic Orthopedic Implants: Materials, Structures, And Surface Modifications. *Metals,* Volume 9(9), p. 1004

Bozdag, M., Karaman, G., 2021. Virtual Morphometry of the First Lumbar Vertebrae for Estimation of Sex Using Computed Tomography Data in the Turkish Population. *Cureus*, Volume 13(7), p. 16597

Clifton, W., Nottmeier, E., Damon, A., Dove, C., Chen, S.G., Pichelmann, M. (2019). A Feasibility Study for the Production of Three-dimensional-printed Spine Models Using Simultaneously Extruded Thermoplastic Polymers. *Cureus*, Volume 11(4), p. 4440

Frost, B.A., Camarero-Espinosa, S., Foster, E.J., 2019. Materials for the Spine: Anatomy, Problems, and Solutions. *Materials*, Volume 12(2), p. 253

Gama, N.V., Ferreira, A., Barros-Timmons, A., 2018. Polyurethane Foams: Past, Present, And Future. *Materials*, Volume 11(10), p. 1841

Genisa, M., Shuib, S., Rajion, Z.A., Mohamad, D., Arief, E.M., 2020. Dental Implant Monitoring Using Resonance Frequency Analysis (RFA) and Cone Beam Computed Tomography (CBCT) Measurement. *International Journal of Technology*, Volume 11(5), pp. 1015–1024

Gopinathan, A., Jerz, J., Kováčik, J., Dvorák, T., Orovčík, L., 2021. Study Of Internal Porous Structure Formation of The Powder Metallurgically Prepared Aluminium Foam. *Journal of Physics: Conference Series*, Volume 2045(1), p. 012003

Hadisujoto, B., Wijaya, R., 2021). Development and Accuracy Test of a Fused Deposition Modeling (FDM) 3D Printing using H-Bot Mechanism. *Indonesian Journal of Computing, Engineering and Design (IJoCED)*, Volume 3(1), pp. 46–53

Hanon, M.M., Zsidai, L., Ma, Q., 2021. Accuracy Investigation of 3D Printed PLA With Various Process Parameters and Different Colors. In: *Materials Today: Proceedings*, Volume 42, pp. 3089–3096

Haque, S.S., 2020. *Minimizing Stringing Issues In FDM Printing. Department of Mechanical and Production Engineering,* Ahsanullah University of Science and Technology (AUST), Dhaka, Bangladesh

Izmin, N.A.N., Hazwani, F., Todo, M., Abdullah, A.H., 2020. Risk of Bone Fracture in Resurfacing Hip Arthroplasty at Varus and Valgus Implant Placements. *International Journal of Technology*, Volume 11(5), pp. 1025–1035

Jackovich, D., O'Toole, B., Hawkins, M.C., Sapochak, L., 2005. Temperature And Mold Size Effects On Physical And Mechanical Properties Of A Polyurethane Foam. *Journal of Cellular Plastics*, Volume 41(2), pp. 153–168

Kong, L., Ma, Y., Ren, M., Xu, M., Cheung, C., 2020. Generation and Characterization of Ultra-Precision Compound Freeform Surfaces. *Science Progress*, Volume 103(1), pp. 1–21

Lewandrowski, K.U., Soriano-Sánchez, J.A., Zhang, X., Ramírez-León, J.F., Soriano Solis, S., Rugeles Ortíz, J.G., Alonso Cuéllar, G.O., de Lima e Silva, M.S., Hellinger, S., Dowling, Á., Prada, N., Choi, G., Datar, G., Yeung, A., 2020. Surgeon Training and Clinical Implementation of Spinal Endoscopy in Routine Practice: Results of a Global Survey. *Journal of Spine Surgery*,Volume 6, p. 237–248

Lyashenko, V., Matarneh, R., Sotnik, S., 2018. Defects of Casting Plastic Products: Causes, Recurrence, Synthesis and Ways of Elimination. International of Modern Engineering Research, Volume 8(2), pp. 1–11

Mondal, N.R., Rafiquzzaman, M., Siddique, M.A., Islam, S. (2020). Optimization of Investment

Casting Parameters to Improve the Mechanical Properties by Taguchi Method. *American Journal of Mechanical and Industrial Engineering*, Volume 5(5), pp. 64–70

Montero, J., Vitale, P., Weber, S., Bleckmann, M., Paetzold, K., 2020. Indirect Additive Manufacturing Of Resin Components Using Polyvinyl Alcohol Sacrificial Moulds. *Procedia CIRP*, Volume 91, pp. 388–395

Mwema, F.M., Akinlabi, E.T., 2020). Basics of Fused Deposition Modelling (FDM). *Fused Deposition Modeling*, Volume 1, pp. 1–15

Nadhif, M.H., Irsyad, M., Rahyussalim, A.J., Utomo, M.S., 2021. Geometrical Evaluation Of CAM-Configured Thermoplastic Polyurethane Lattices For Intervertebral Disc Replacements. *In*: AIP Conference Proceedings, Volume 2382 (1), *p. 030006*

Rampf, M., Speck, O., Speck, T., Luchsinger, R.H., 2011. Structural and Mechanical Properties of Flexible Polyurethane Foams Cured Under Pressure. *Journal of Cellular Plastics,* Volume *48*(1), pp. 53–69

Rani, A.M.A., Fua-Nizan, R., Din, M.Y., 2017. Manufacturing Methods For Medical Artificial Prostheses– A Review. *Malaysian Journal of Fundamental and Applied Sciences*, Volume 13, pp. 464–469

Saptaji, K., Afiqah, S.N., Ramdan, R.D., 2019. A Review on Measurement Methods for Machining Induced Residual Stress. *Indonesian Journal of Computing, Engineering and Design (IJoCED)*, Volume 1(2), pp. 106–120

Saptaji, K., Hardiyasanti, D.C., Ali, M. F., Frandito, R., Dewi, T.K., 2022. Potential Applications of Hydroxyapatite-Mineralized-Collagen Composites as Bone Structure Regeneration: a Review. *Journal of Science and Applied Engineering*, Volume 5(1), p. 3577

Shim, V., Boheme, J., Josten, C., Anderson, I., 2012. Use of Polyurethane Foam in Orthopaedic Biomechanical Experimentation and Simulation. In: *Polyurethane,* pp. 171–200

Sidek, N., Bakar, I.A.A., Azman, A.A., Rahman, A.S.A., Austin, W.A., 2017. Strength Characteristic of Polyurethane With Variation of Polyol to Isocyanate Mix Ratio : A Numerical Analysis. *In*; Proceedings - 2017 IEEE 2nd International Conference on Automatic Control and Intelligent Systems (I2CACIS), pp. 31–34

Singh, R., Singh, S., Singh, G., 2014. Dimensional Accuracy Comparison of Investment Castings Prepared with Wax and ABS Patterns for Bio-medical Application. *Procedia Materials Science*, Volume 6, pp. 851–858

Standard Test Method for Apparent Density of Rigid Cellular Plastics 1 This international standard was developed in accordance with internationally recognized principles on standardization established in the Decision on Principles for the Development of I. (2020). 4–7. https://doi.org/10.1520/D1622-14.2

Tagami, T., Fukushige, K., Ogawa, E., Hayashi, N., Ozeki, T., 2017. 3D Printing Factors Important For The Fabrication Of Polyvinylalcohol Filament-Based Tablets. *Biological and Pharmaceutical Bulletin*, Volume 40(3), pp. 357–364

Wong, H.H.C., Kwan, A.K.H., 2008. Packing Density Of Cementitious Materials: Part 1-Measurement Using A Wet Packing Method. *Materials and Structures/Materiaux et Constructions*, Volume 41(4), pp. 689–701